HAYATI
Journal of Biosciences

Vol. 33 No. 1, January 2026 232-239
DOI:10.4308/hjb.33.1.232-239
ISSN: 1978-3019
EISSN: 2086-4094

Research Article

Check for updates

OPEN ACCESS

Evaluation of Curcumin-derived Carbon-dots' Inhibitory Activity as SARS-CoV-2 Antiviral Candidate Using Chemical Crosslinking

Audrey Angelina Putri Taharuddin[1], Nicholas Yamahoki[1], Rebecca Stephanie[1], Dian Fitria Agustiyanti[2], Popi Hadi Wisnuwardhani[2], Marissa Angelina[3], Yana Rubiyana[2], Ratih Asmana Ningrum[2], Andri Wardiana[2], Desriani Desriani[2], Hariyatun Hariyatun[2], Ferry Iskandar[4,5,6], Fitri Aulia Permatasari[5,6,7], Ernawati Arifin Giri-Rachman[1], Azzania Fibriani[1*]

[1]*School of Life Sciences and Technology, Institut Teknologi Bandung, Bandung 40132, Indonesia*
[2]*Research Center for Genetic Engineering, Indonesian National Research and Innovation Agency (BRIN), Cibinong 16911, Indonesia*
[3]*Research Center for Pharmaceutical Ingredients and Traditional Medicine, Indonesian National Research and Innovation Agency (BRIN), Serpong 15314, Indonesia*
[4]*Research Center for Nanoscience and Nanotechnology, Institut Teknologi Bandung, Bandung 40132, Indonesia*
[5]*Department of Physics, Faculty of Mathematics and Natural Sciences, Institut Teknologi Bandung, Bandung 40132, Indonesia*
[6]*Collaboration Research Center for Advanced Energy Materials, National Research and Innovation Agency, Institut Teknologi Bandung, Bandung 40132, Indonesia*
[7]*Research Center for Chemistry, National Research and Innovation Agency (BRIN), Serpong 15314, Indonesia*

ARTICLE INFO

Article history:
Received August 27, 2025
Received in revised form September 2, 2025
Accepted September 24, 2025
Available Online October 24, 2025

KEYWORDS:
Antiviral,
Carbon-dots,
Curcumin,
Chemical Crosslinking,
Nucleocapsid,
SARS-CoV-2

Copyright (c) 2026 @author(s).

ABSTRACT

In our previous work, we demonstrated that curcumin-derived carbon dots (Cur-CDs) have potential as antivirals for COVID-19. However, the precise mechanism of action remains unclear. This study investigated the potential of Cur-CDs against SARS-CoV-2 by targeting the dimerization of the C-terminal domain of nucleocapsid protein (N-CTD) using chemical crosslinking. Recombinant SARS-CoV-2 N-CTD was expressed, purified, and subjected to chemical crosslinking. The dimerization inhibition ability of Cur-CDs was assessed with ligand concentrations ranging from 0 to 2,000 µg/mL. Successful inhibition —defined as a noticeable reduction in SARS-CoV-2 N-CTD dimer band intensity on SDS-PAGE—was observed when Cur-CDs were present at 8 to 16 times the protein concentration. We hypothesize that Cur-CDs bind to the dimerization residues, preventing non-covalent interactions between monomers and limiting dimer formation. Our findings suggest that Cur-CDs could be a promising antiviral strategy for SARS-CoV-2, especially targeting the dimerization of the nucleocapsid protein. Additionally, this study also highlights the use of chemical crosslinking as a valuable tool for interaction-based drug screening.

1. Introduction

Since May 5th, 2023, the World Health Organization (WHO) officially lifted the Public Health Emergency of International Concern (PHEIC) status from Coronavirus Disease 2019 (COVID-19) (International Institute for Sustainable Development 2023). However, as an RNA virus, Severe Acute Respiratory Syndrome Coronavirus 2 (SARS-CoV-2) is known for its high mutation rate, which can contribute to the emergence of new variants (Mótyán *et al.* 2022). The presence of non-synonymous mutations can alter amino acid residues in the antiviral's target protein, which in turn may influence the binding affinity between the protein and the antiviral targets. Additionally, there is the potential for a decrease in the effectiveness of existing antivirals (Chu & Wei 2019; Sedighpour & Taghizadeh 2022). Therefore, the exploration of antivirals with high specificity and efficiency is essential as a preventive measure against the possibility of future pandemics.

* Corresponding Author
E-mail Address: afibriani@itb.ac.id

In our previous research, we demonstrated that curcumin-derived carbon dots (Cur-CDs) (Figure 1) have potential as antivirals for COVID-19, as shown by a viral infectivity assay. Using molecular docking, we also demonstrated that Cur-CDs exhibit a high binding affinity towards the C-terminal domain (CTD) of the SARS-CoV-2 nucleocapsid (N) protein (Fibriani *et al.* 2023). Carbon-dots (CDs) are carbon-based nanomaterials characterized by high solubility, biocompatibility, and photoluminescence. CDs are typically spherical and less than 10 nm in size (Shafi *et al.* 2020). CDs synthesized from bioactive compounds (e.g., curcumin, flavonoids) often exhibit unique characteristics when used as precursors. These compounds undergo structural changes while retaining their functional surface groups, which enhances their solubility and antiviral properties (Lin *et al.* 2019; Wu *et al.* 2022). Although we have demonstrated its antiviral potential, it remains unclear whether the positive results were due to the inhibition of N protein dimerization or interactions with another protein (Contreras-Llano & Tan 2018). Therefore, further validation is necessary to confirm the interaction between Cur-CDs and the target protein, SARS-CoV-2 N-CTD.

Validation can be performed using chemical crosslinking, a technique that covalently joins two or more molecules, either intramolecularly or intermolecularly, using a crosslinker (Arora *et al.* 2017). Crosslinkers can only bind molecules that are in close proximity due to non-covalent interactions (Tang & Bruce 2009). This method was utilized by Furuta *et al.* (2005) to evaluate an antibacterial compound targeting the dimerization of the histidine kinase (HK) YycG. Similarly, Putra (2015) also adapted the method to target the dimerization of PhoR from *Mycobacterium tuberculosis*. The basis of the validation lies in the compound's ability to inhibit non-covalent interactions between proteins, such as the interaction between two monomers, thereby preventing the crosslinker from joining the monomers. The results of crosslinking can be analyzed using SDS-PAGE (Furuta *et al.* 2005). In this research, chemical crosslinking will specifically target the dimerization domain of the SARS-CoV-2 N protein.

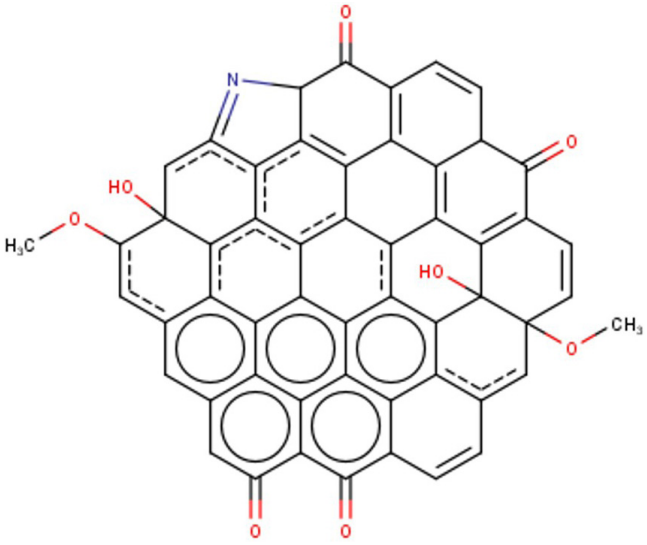

Figure 1. Hypothetical structure of Cur-CDs. As N-doped carbon dots, Cur-CDs are proposed to exist in pyrrolic form. Red indicates chemical bonds formed with oxygen, while blue indicates chemical bonds formed with nitrogen

This study aimed to validate the potential of Cur-CDs to bind to SARS-CoV-2 N-CTD and to inhibit its dimerization, while also providing a basis for understanding the interactions between Cur-CDs and the SARS-CoV-2 N-CTD.

2. Materials and Methods

2.1. Expression Vector and Bacterial Host

The *Escherichia coli* BL21 (DE3) strain containing the SARS-CoV-2 N-CTD expression vector (pET23a_CTD N) was established and obtained from our laboratory collection. The protein was designed to be conjugated with a 6xHis-tag on its C-terminus to facilitate purification. The bacterial culture was maintained in Luria-Bertani (LB) agar medium supplemented with 100 µg/mL ampicillin and subcultured every two weeks. The bacterial stock was stored at −80°C. All maintenance and experimental procedures were conducted at the School of Life Sciences and Technology, Institut Teknologi Bandung, Indonesia.

2.2. Expression Vector and Bacterial Host

Cur-CDs were synthesized using a solvothermal approach, as described in Fibriani *et al.* (2023). Cur-CDs powder was obtained after freeze-drying and dissolved in sterile distilled water to a stock concentration of 10,000 µg/mL. For the compound inhibitory assay, Cur-CDs stock solution was diluted to final concentrations of 100, 500, 1,000, 1,500, and 2,000 µg/mL.

2.3. Insert Gene Confirmation of Recombinant *E. coli* BL21 (DE3)

The presence of SARS-CoV-2 N-CTD gene was confirmed with colony PCR using T7 universal primer and N-CTD specific primer (Forward: 5'-CATATGATGACCAAAAAATCTGCTGC-3';

Reverse: 5'-CTCGAGCGGGAAGGTTTTGTAAG-3'). The plasmid from positive colonies was then isolated using Presto™ Mini Plasmid (Geneaid Biotech Ltd., Cat No. PDH300, Taiwan). Confirmation of the DNA sequence was done using Sanger sequencing against T7 universal primer, followed by pairwise alignment using EMBOSS WATER (https://www.ebi.ac.uk/jdispatcher/psa/emboss_water).

2.4. *In Silico* Study: SARS-CoV-2 N-CTD Physicochemical Properties

Physicochemical properties were analyzed *in silico* using ExPASy ProtParam (https://web.expasy.org/protparam/). Properties identified are molecular weight, pI value, atomic composition, half-life estimation, instability index, and Grand Average of Hydropathicity (GRAVY).

2.5. Recombinant SARS-CoV-2 N-CTD Expression

Protein expression was performed by culturing recombinant *E. coli* BL21 (DE3) (10% (v/v) inoculum) in LB broth supplemented with 100 µg/mL ampicillin at 37°C with 150 rpm agitation. The culture was grown until the optical density (OD_{600}) reached 0.6 (mid-log phase). Then, protein expression was induced by adding 0.25 mM isopropyl β-D-1-thiogalactopyranoside (IPTG), and the culture was incubated at 37°C with agitation at 150 rpm for 3 hours.

The culture was harvested by centrifugation (6000 x g, 4°C) for 5 minutes. Each 0.02 grams of cell pellet was resuspended in 100 µL of native binding buffer (PBS 1X, 1 mM PMSF, 10 mM imidazole). Fractionation was performed by sonication using the Omni Ruptor 4000 ultrasonic homogenizer (Omni International, USA) (30% power, 30% pulse, 5 minutes), followed by centrifugation (13000 x g, 4°C) for 15 minutes. The resulting supernatant was collected as the soluble fraction. The protein concentration was determined using a UV-Vis Spectrophotometer Nanodrop™ (Thermo Scientific Inc., USA). The protein profile was analyzed using SDS-PAGE at 150 V (±90 minutes), using a 12.5% Tris-glycine buffer system. At this step, *E. coli* BL21 (DE3) without the SARS-CoV-2 N-CTD expression system was used as a negative control.

2.6. Recombinant SARS-CoV-2 N-CTD Purification

Recombinant protein was purified based on 6xHis-tag affinity chromatography using HisPur™ Ni-NTA Spin Columns (Thermo Scientific, Cat No. 88225, USA).

Prior to purification, the column was equilibrated with 1x volume of resin beads in native binding buffer. The column was then centrifuged (700 x g, 4°C) for 2 minutes. After equilibration, the soluble fraction was poured into the column and incubated in a 360° rotating shaker at 4°C for 2 hours. After incubation, the column was centrifuged (700 x g, 4°C) for 2 minutes. The "Washing" step was carried out 15 times with three different concentrations of imidazole in native wash buffer (PBS 1X, imidazole) at 25 mM, 35 mM, and 45 mM. The imidazole concentration was varied every 5 washes. After washing, protein was eluted with a 1x volume of resin beads in native elution buffer (PBS 1X, imidazole 250 mM). The presence of the protein was confirmed with SDS-PAGE at 150 V (±90 minutes), using a 12.5% Tris-glycine buffer system. The purified recombinant protein was then concentrated by precipitation using a 1:4 cold acetone solution.

2.7. Chemical Crosslinking of SARS-CoV-2 N-CTD

Chemical crosslinking was performed by mixing equal volumes of concentrated 150 µM SARS-CoV-2 N-CTD and BS^3 (bis(sulfosuccinimidyl)suberate) crosslinker in conjugation buffer (1X PBS). The reaction was incubated on ice for 2 hours and subsequently quenched by adding glycine 1 M to a final concentration of 100 mM. The quenching reaction was incubated at room temperature for 15 minutes. Various crosslinker concentrations were tested, including 0, 0.3, 0.6, and 1.2 mM. The success of crosslinking was assessed using SDS-PAGE at 150 V (±90 minutes), using a 12.5% Tris-glycine buffer system.

Western blotting was conducted to confirm further the ability of chemical crosslinking to dimerize two monomers. The blotting process was performed using a semi-wet transfer method with the eBlot® L1 Protein Transfer System (GenScript Inc., USA) and an antibody targeting the 6X His-tag. Protein visualization was achieved using the WesternSure® PREMIUM Chemiluminescent Substrate (LI-COR Inc., USA) and imaged with the C-Digit® Blot Scanner (LI-COR Inc., USA).

2.8. Validation of Compound Inhibition Ability with Chemical Crosslinking

Validation was conducted by reacting 20 µL of 150 µM of SARS-CoV-2 N-CTD with 5 µL of Cur-CDs at varying concentrations. The tested Cur-CDs concentrations were 0 µg/mL, 100 µg/mL, 500 µg/mL,

1,000 µg/mL, 1,500 µg/mL, and 2,000 µg/mL. The reaction mixtures were incubated at 37°C for 1 hour. Subsequently, chemical crosslinking was performed using the method described previously. At this stage, a crosslinking negative control without BS^3 was also included. After SDS-PAGE analysis, the intensity of the protein bands was quantified using ImageJ software (Abramoff *et al.* 2004). The band intensity was calculated as integrated density and expressed as the percentage of the target protein relative to the total protein:

$$\%\ \text{target protein: total protein} = \frac{\text{Density of target protein band} - \text{Density of protein lane band}}{\text{Density of protein lane band}} \times 100$$

2.9. Data and Statistical Analysis

Data processing and statistical analysis were performed using ImageJ for quantification, Microsoft Excel (Microsoft, USA), and SPSS Statistics (IBM, USA). The data were presented as mean ± standard deviation from three repetitions. First, a normality test was performed using the Shapiro-Wilk test for each test group, where $p>0.05$ was considered indicative of a normal data distribution. Data with a normal distribution were analyzed for significance using one-way ANOVA, followed by post-hoc analysis using Tukey's test, where $p\leq0.05$ was considered statistically significant.

3. Results

3.1. Confirmation of SARS-CoV-2 N-CTD Gene in Recombinant *E. coli* BL21 (DE3)

The presence of the SARS-CoV-2 N-CTD expression system was confirmed in two recombinant *E. coli* BL21 (DE3) colonies (Figure 2). This result was indicated by the presence of target genes, as detected using both the T7 universal primer and the insert-specific primer, N-CTD. The T7 universal primer covers the entire region encompassing the T7P, N-CTD gene, 6×His-tag, and T7T, whereas the N-CTD-specific primer only covers the N-CTD gene. Additionally, an excess plasmid of approximately 3950 bp was also observed.

Further confirmation was conducted by sequencing plasmids from both colonies using the T7 universal primer. The sequencing results revealed 98.6% similarity to the N-CTD sequence from the SARS-CoV-2 whole-genome reference sequence (GenBank: NC_045512). The remaining 1.4% dissimilarity was attributed to five point mutations: c.26A>T, c.27G>C, c.63G>T, c.150C>T, and c.249C>T.

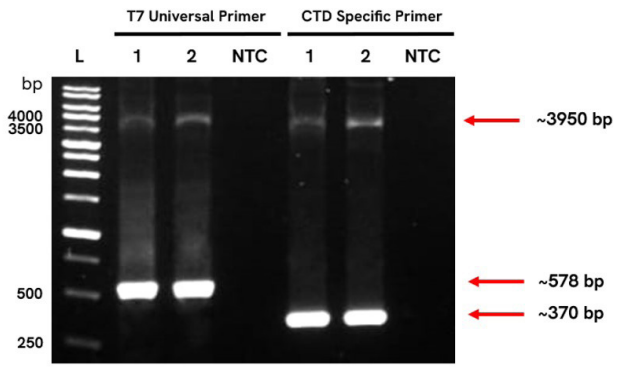

Figure 2. Electropherogram of colony PCR from colony numbers 1 and 2. Both colonies contained the gene of interest. L = 1 kb DNA ladder; NTC = no template control. 1% agarose, TAE 1X, 100V

Additional protein sequence alignment analysis was performed using the EMBOSS Water tool (https://www.ebi.ac.uk/jdispatcher/psa/emboss_water) against the reference protein sequence. The alignment showed 100% similarity to the reference sequence, indicating that the mutations were synonymous. Moreover, the sequencing results confirmed the correct orientation of the gene within the plasmid.

3.2. Physiochemical Characterization of Recombinant SARS-CoV-2 N-CTD

Based on *in silico* characterization, SARS-CoV-2 N-CTD conjugated with 6xHis-tag has a molecular weight of 14.5 kDa and a pI of 9.65. The half-life estimation was determined based on the N-terminus amino acid residue, which is methionine. This result suggests that the protein would remain stable for more than 10 hours inside *E. coli* before degradation. Additionally, the instability index, with a value greater than 40, indicates that the protein is stable outside the host. Another parameter analyzed was the GRAVY score, which showed a negative value, indicating that the protein is hydrophilic and is likely to be found in the soluble fraction or cytoplasm. The parameters and their respective values are summarized in Table 1.

3.3. Expression and Purification of Recombinant SARS-CoV-2 N-CTD

The SARS-CoV-2 N-CTD protein was detected at ~14.5 kDa, consistent with our physicochemical analysis, in the elution fractions from recombinant *E. coli* BL21 (DE3) (Figure 3A). However, a native protein from *E. coli* BL21 (DE3) was also observed at a similar size (data not shown). When the elution fractions were compared, the target protein was exclusively detected

Table 1. Physiochemical characteristics of SARS-CoV-2 N-CTD based on *in silico* analysis

Parameters	Results
Molecular weight	14567.45 Da (14.5 kDa)
pI	9.65
Atomic composition	$C_{649}H_{997}N_{189}O_{187}S_4$
Half-time estimation	30 hours (mammalian reticulocytes, *in vitro*)
	>20 hours (yeast, *in vivo*)
	>10 hours (*E. coli, in vivo*)
Instability index	28.04
GRAVY	-0.859

in the elution fractions from recombinant *E. coli* BL21 (DE3) (Figures 3A and B), verifying its expression.

3.4. Chemical Crosslinking of SARS-CoV-2 N-CTD

The addition of 0.3-1.2 mM crosslinker successfully facilitated the dimerization of SARS-CoV-2 N-CTD monomers in close proximity. This was evidenced by the presence of a monomer protein band (~14.5 kDa) and a second band at approximately twice the size (~29 kDa), corresponding to the dimer protein (Figure 4). The ~29 kDa protein band was absent in the negative control sample without the BS^3 crosslinker, confirming the successful formation of dimer proteins through chemical crosslinking. Since no differences in protein band patterns were observed across the BS^3 concentrations tested, we selected the lowest concentration, 0.3 mM, for further subsequent experiments.

Western blotting analysis was then performed to ensure the success of chemical crosslinking using an anti-His-tag antibody that binds to the polyhistidine residue in the protein. The analysis revealed that the antibody bound to the polyhistidine residue in both the monomers (~14.5 kDa) and dimers (~29 kDa) of the SARS-CoV-2 N-CTD (Figure 5). Therefore, we can conclude that the protein bands in the SDS-PAGE of the chemical crosslinking were indeed monomer and dimer of SARS-CoV-2 N-CTD.

3.5. Validation of Cur-CDs' Dimerization Inhibition Ability with Chemical Crosslinking

The use of Cur-CDs at concentrations of 1,000 µg/mL and above effectively reduced the chemical crosslinking ability to produce the dimeric protein (~29 kDa) (Figure 6). This result was also supported by the quantification of protein band density using ImageJ (Table 2). As the concentration of Cur-CDs increased, the density of the dimer protein band decreased, approaching the level observed in the negative control

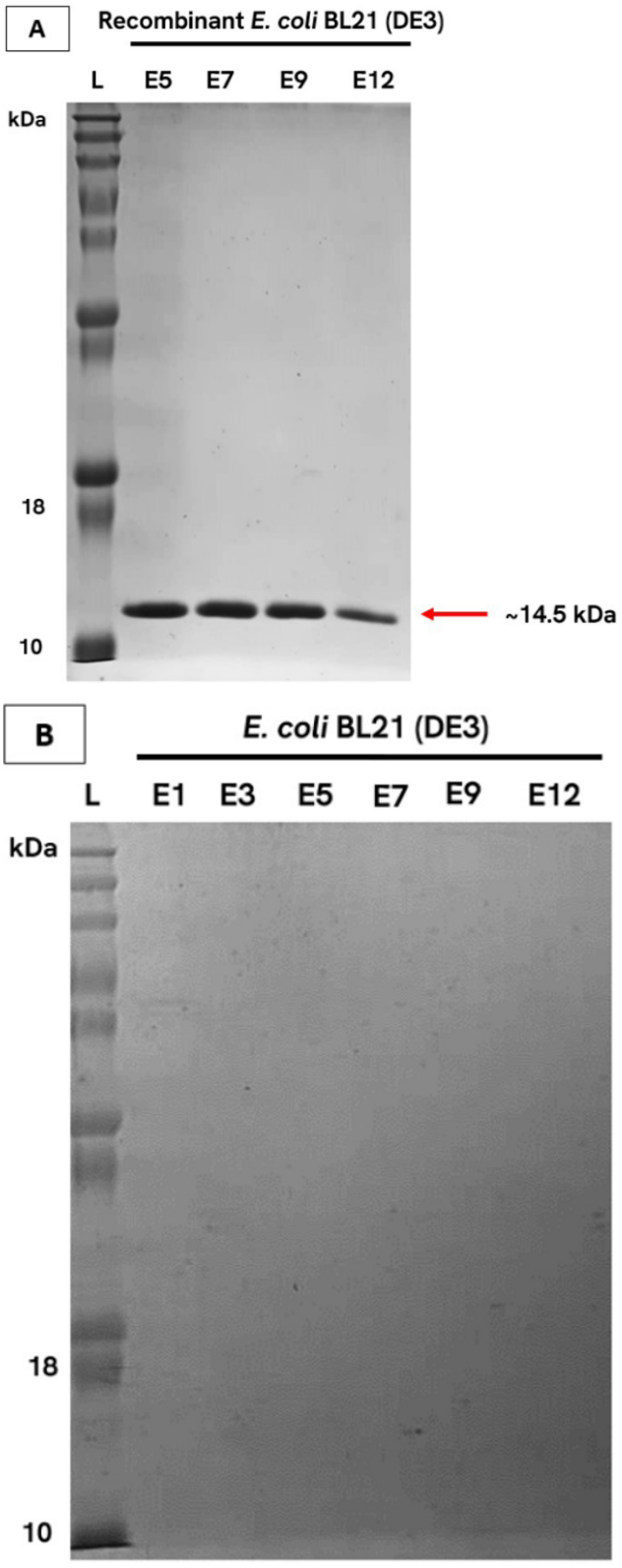

Figure 3. Electropherogram of SARS-CoV-2 N-CTD purification based on Ni-NTA affinity chromatography from (A) recombinant *E. coli* BL21 (DE3) and (B) *E. coli* BL21 (DE3) without the expression system. SARS-CoV-2 N-CTD has a size of 14.5 kDa. L = prestained protein ladder; E = elution fraction. Tris-glycine 12.5%, 150V

(without crosslinker). This decrease was particularly pronounced when the ligand concentration was 8 to 16 times higher than that of the protein.

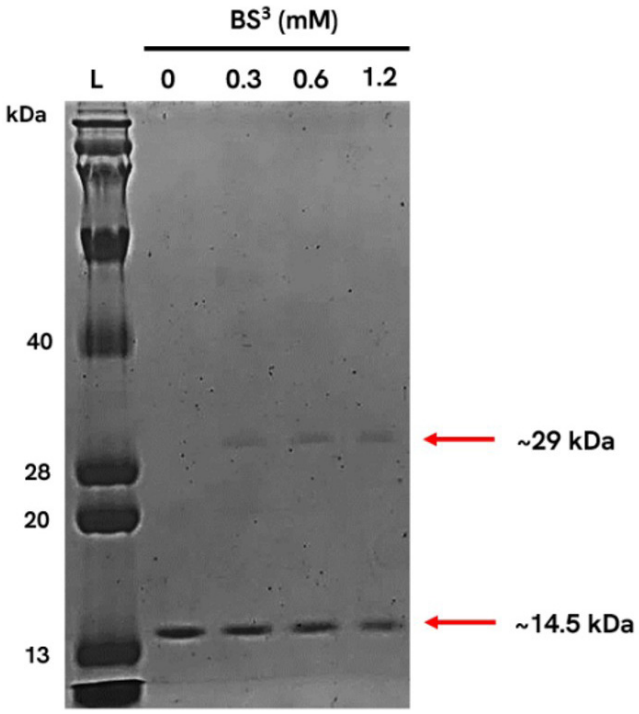

Figure 4. Electropherogram of SARS-CoV-2 N-CTD chemical crosslinking with 0-1.2 mM BS³ crosslinker. Monomer and dimer have a size of 14.5 kDa and 29 kDa, respectively. L = prestained protein ladder. Tris-glycine 12.5%, 150V, 3 replicates

4. Discussion

This study demonstrated the ability of Cur-CDs to inhibit the dimerization of the SARS-CoV-2 N protein, modelled by its dimerization domain (CTD). SARS-CoV-2 N-CTD was successfully expressed using 0.5 mM IPTG induction (Figure 3). However, the presence of a native protein band of similar size posed a challenge

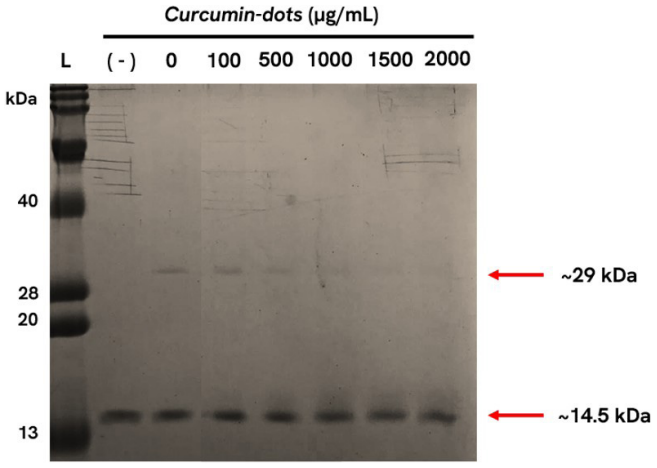

Figure 6. Electropherogram of dimerization inhibition ability of 0-2,000 µg/mL Cur-CDs using chemical crosslinking. Monomer and dimer have a size of 14.5 kDa and 29 kDa, respectively. L = prestained protein ladder; (-): negative control (without BS3). Tris-glycine 12.5%, 150V. Summary of band density (%ratio of protein: lane) from ImageJ is presented in Table 2

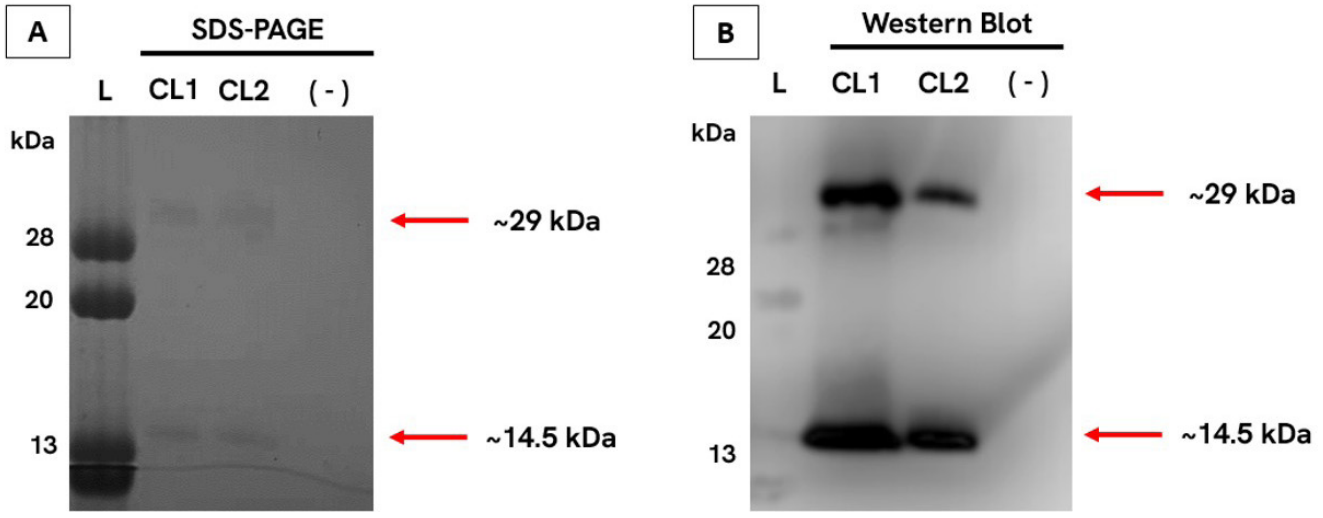

Figure 5. SDS-PAGE (A) and western blotting (B) analysis of SARS-CoV-2 N-CTD chemical crosslinking using 0.3 mM BS³ crosslinker. Monomer and dimer have a size of 14.5 kDa and 29 kDa, respectively. L = prestained protein ladder; CL = chemical crosslinking sample; (-) = negative control of *E. coli* BL21 (DE3)

Table 2. SDS-PAGE band density (%ratio of protein: lane) on dimerization inhibition ability of 0-2000 µg/mL of Cur-CDs using chemical crosslinking. Data were presented as mean ± SD (n = 21). ANOVA One-way, Tukey Test

Cur-CDs concentrations (µg/mL)	%Ratio of protein: lane (%)*
Negative control	2.36303295[a]
0	4.06093752[b]
100	4.04943763[b]
500	3.54835635[ab]
1,000	3.12722647[ab]
1,500	2.8029859[a]
2,000	2.5219839a

in identifying and confirming the target protein. The native protein is suspected to be a histone-like protein involved in folding genetic material into the nucleoid. This protein group includes DNA-binding protein (HU), integration host factor (IHF), and histone-like nucleoid structuring protein (H-NS), with sizes ranging from 10 to 15 kDa (Savitskaya *et al.* 2018).

Crosslinking was performed using BS^3, a homobifunctional crosslinker that contains two N-hydroxysulfosuccinimide (NHS) ester groups, which can react with amino groups on proteins (Shi *et al.* 2017). BS^3 offers several advantages over glutaraldehyde, including the production of fewer side products, good reaction specificity, and ensuring the stability of the resulting crosslinked products (Belsom & Rappsilber 2021). In this research, crosslinking was performed at a neutral pH of 7.4, where SARS-CoV-2 N-CTD is known to exist in equilibrium between monomeric and dimeric forms (Zhao *et al.* 2021). This condition increases the likelihood of monomers being in close proximity, thereby facilitating efficient crosslinking. However, no significant differences in monomer and dimer protein bands were observed across the various concentrations that we used (Figure 4). Similar research by Shi *et al.* (2017) also demonstrated that varying concentrations of 0.3–1.2 mM BS^3 had minimal effects on the crosslinking of amyloid-β peptide (Aβ) oligomers. We hypothesize that further optimization may not be effective in increasing crosslinking efficiency. Crosslinkers that target Lys residues, such as BS^3, are known for their high reactivity and specificity. However, it yields a relatively small amount of product due to the requirement for Lys residues to be in close proximity for successful crosslinking (Gomes & Gozzo 2010). Although the reaction did not yield the expected improvements, we successfully achieved dimerization of the protein. Therefore, we are confident in proceeding with the subsequent analyses.

The dimerization inhibition ability of Cur-CDs on SARS-CoV-2 N-CTD was assessed using Cur-CD concentrations ranging from 0 to 2,000 µg/mL. This range differs from our previous research, which utilized concentrations between 0 and 10 µg/mL (Fibriani *et al.* 2023). Typically, it is recommended to use ligand concentrations within the dissociation constant (KD) range of the protein (Bio-Rad Laboratories Inc., 2013). However, this research has not yet determined the KD of the protein-ligand interaction. Furuta *et al.* (2005) successfully used a crosslinking method to screen 1000 µg/mL of the I-8-15 compound with 100 pmol of N100-CyycG protein, where the compound concentration was 3,600 times higher than the protein. Therefore, we also decided to use Cur-CDs concentrations up to 2,000 µg/mL to represent ligand concentrations approximately 10 to 20 times higher than the protein concentration. This approach was chosen to ensure ligand saturation at the protein binding sites (Wa 2024).

Our research demonstrated successful inhibition when Cur-CD concentrations were 8 to 16 times higher than the protein concentration, which is still within the intended range of 10 to 20 (Figure 6). Inhibition was considered successful when a clear reduction in SARS-CoV-2 N-CTD dimer formation was observed in SDS-PAGE, indicated by a diminished dimer band intensity compared to the control. Statistical analysis of the SDS-PAGE band density (Table 2) also showed that, with increasing Cur-CDs concentration, the band density was not significantly different from the negative control. This further supports the idea that Cur-CDs inhibit the crosslinking reaction. We hypothesize that as the concentration of Cur-CDs increases, more compounds bind to the SARS-CoV-2 N-CTD, particularly at the dimerization residues. This observation aligns with our previous research, which demonstrated that Cur-CDs have a high affinity for the dimerization residues, as determined by molecular docking (Fibriani *et al.* 2023). As Cur-CDs bind to these residues, the two monomers were unable to interact non-covalently, preventing them from coming into close proximity to be joined by the crosslinker. Consequently, the formation of the dimer protein becomes limited.

In summary, this study demonstrated a potential mechanism of Cur-CDs as an antiviral agent against SARS-CoV-2, targeting the nucleocapsid protein by inhibiting the non-covalent interactions between monomers that are necessary for dimer formation. Additionally, this study showcased the application of chemical crosslinking for interaction-based drug

screening. Future studies could explore the use of this method for other diseases or target proteins. However, further optimization may be needed.

Acknowledgements

This research was funded by the Indonesian National Research and Innovation Agency (BRIN), RIIM Biologi Struktur Biomolekul Keanekaragaman Hayati, grant number 45/III.5/HK/2024

References

Abramoff, M.D., Magalhaes, P.J., Ram, S.J., 2004. Image processing with ImageJ. *Biophotonics International.* 11, 36-42.

Arora, B., Tandon, R., Attri, P., Bhatia, R. 2017. Chemical crosslinking: role in protein and peptide science. *Curr Protein Pept Sci.* 18, 946-955. https://doi.org/10.2174/1389203717666160724202806 International Institute for Sustainable Development, 2023. WHO declares end to COVID-19 as global health emergency Available at: https://sdg.iisd.org/news/who-declares-end-to-covid-19-as-global-health-emergency/ [Date accessed: 21 July 2024].

Belsom, A., Rappsilber, J., 2021. Anatomy of a crosslinker. *Curr Opin Chem Biol.* 60, 39-46. https://doi.org/10.1016/j.cbpa.2020.07.008

Bio-Rad Laboratories, Inc. 2013. Protein Interaction Analysis Available at: https://www.biorad.com/webroot/web/pdf/lsr/literature/Bulletin_5538.pdf. [Date accessed: 10 April 2024].

Chu, D., Wei, L. 2019. Non-synonymous, synonymous and nonsense mutations in human cancer-related genes undergo stronger purifying selections than expectation. *BMC Cancer* 19, 359. https://doi.org/10.1186/s12885-019-5572-x

Contreras-Llano, L.E., Tan, C., 2018. High-throughput screening of biomolecules using cell-free gene expression systems. *Synthetic Biology.* 3, ysy012. https://doi.org/10.1093/synbio/ysy012

Fibriani, A., Taharuddin, A.A.P., Stephanie, R., Yamahoki, N., Laurelia, J., Wisnuwardhani, P.H., Agustiyanti, D.F., Angelina, M., Rubiyana, Y., Ningrum, R.A., Wardiana, A., Iskandar, F., Permatasari, F.A., Giri-Rachman, E.A., 2023. Curcumin-derived carbon-dots as a potential COVID-19 antiviral drug. *Heliyon.* 9, e20089. https://doi.org/10.1016/j.heliyon.2023.e20089

Furuta, E., Yamamoto, K., Tatebe, D., Watabe, K., Kitayama, T., Utsumi, R., 2005. Targeting protein homodimerization: a novel drug discovery system. *FEBS Lett.* 579, 2065-2070. https://doi.org/10.1016/j.febslet.2005.02.056

Gomes, A.F., Gozzo, F.C., 2010. Chemical crosslinking with a diazirine photoactivatable crosslinker investigated by MALDI- and ESI-MS/MS. *J Mass Spectrom.* 45, 892-899. https://doi.org/10.1002/jms.1776

International Institute for Sustainable Development, 2023. WHO declares end to COVID-19 as global health emergency Available at: https://sdg.iisd.org/news/who-declares-end-to-covid-19-as-global-health-emergency/ [Date accessed: July 21st 2024]

Lin, C.J., Chang, L., Chu, H.W., Lin, H.J., Chang, P.C., Wang, R.Y.L., Unnikrishnan, B., Mao, J.Y., Chen, S.Y., Huang, C.C., 2019. High amplification of the antiviral activity of Curcumin through transformation into carbon quantum dots. *Small.* 15, 1902641. https://doi.org/10.1002/smll.201902641

Mótyán, J.A., Mahdi, M., Hoffka, G., Tőzsér, J., 2022. Potential resistance of SARS-CoV-2 main protease (Mpro) against protease inhibitors: lessons learned from HIV-1 protease. *Int. J. Mol. Sci.* 23, 3507. https://doi.org/10.3390/ijms23073507

Putra, R.M., 2015. *Purifikasi Protein Domain Sitoplasmik PhoR Mycobacterium tuberculosis H37Rv untuk Penapisan Anti Tuberkular Baru.* Sekolah Ilmu dan Teknologi Hayati, Institut Teknologi Bandung, Bandung.

Savitskaya, A., Nishiyama, A., Yamaguchi, T., 2018. C-terminal intrinsically disordered region-dependent organization of the mycobacterial genome by a histone-like protein. *Sci Rep.* 8, 8197. https://doi.org/10.1038/s41598-018-26463-9

Sedighpour, D., Taghizadeh, H., 2022. The effects of mutation on the drug binding affinity of Neuraminidase: case study of Capsaicin using steered molecular dynamics simulation. *J Mol Model.* 28, 36. https://doi.org/10.1007/s00894-021-05005-7

Shafi, A., Bano, S., Sabir, S., Khan, M.Z., Rahman, M.M., 2020. *Carbon-Based Material for Environmental Protection and Remediation.* IntechOpen, London.

Shi, J.M., Pei, J., Liu, E., Zhang, L., 2017. Bis(sulfosuccinimidyl) suberate (BS3) crosslinking analysis of the behavior of amyloid-β peptide in solution and in phospholipid membranes. *PLoS One.* 12, e0173871. https://doi.org/10.1371/journal.pone.0173871

Tang, X., Bruce, J.E., 2009. Chemical crosslinking for protein-protein interaction studies. *Methods Mol Biol.* 492, 283-93. https://doi.org/10.1007/978-1-59745-493-3_17

Wa, Y., 2024. Re: How to choose the concentration of protein and ligand for ITC experiment?. Available at: https://www.researchgate.net/post/How_to_choose_the_concentration_of_protein_and_ligand_for_ITC_experiment/65b1d3c0bc2623fa8a0dd5aa/citation/download. [Date accessed: 10 April 2024]

Wu, L., Gao, Y., Zhao, C., Huang, D., Chen, W., Lin, X., Liu, A., Lin, L., 2022. Synthesis of curcumin-quaternized carbon quantum dots with enhanced broad-spectrum antibacterial activity for promoting infected wound healing. *Biomater Adv.* 133, 112608. https://doi.org/10.1016/j.msec.2021.112608

Zhao, H., Wu, D., Nguyen, A., 2021. Energetic and structural features of SARS-CoV-2 N-protein co-assemblies with nucleic acids. *iScience.* 24, 102523. https://doi.org/10.1016/j.isci.2021.102523